HTD-Vol. 171, Heat Transfer in Electronic Equipment
ASME 1991

META – A CONJUGATE HEAT TRANSFER MODEL FOR AIR COOLING OF CIRCUIT BOARDS WITH ARBITRARILY LOCATED HEAT SOURCES

J. R. Culham, T. F. Lemczyk, S. Lee, and M. M. Yovanovich
Department of Mechanical Engineering
Microelectronics Heat Transfer Laboratory
University of Waterloo
Waterloo, Ontario, Canada

Abstract

A conjugate model for air flow over flat plates with arbitrarily located heat sources is developed based on the integral formulation of the boundary layer equations combined with a finite volume solution which assumes two-dimensional heat flow within the plate. The fluid and solid solutions are coupled through an iterative procedure, allowing a unique temperature profile to be obtained at the fluid-solid interface which simultaneously satisfies the temperature field within each domain. Radiation heat loss is also included in the plate heat transfer. A detailed package modeller is also incorporated within the program framework to allow internal package thermal resistances to be determined and give a detailed thermal description for each package with die plane temperatures.

Surface temperature profiles obtained from flat plate circuit board prototypes are used to substantiate the various assumptions inherent in the model and to establish the accuracy of the model for a range of design conditions commonly used in microelectronic applications. Data published in the open literature are also used to show the flexibility of the model to simulate a variety of microelectronic applications.

The model is shown to be in good agreement with the experimental data over a wide range of flow conditions and power levels, and good agreement is achieved with experimental data typical of many microelectronic applications.

Nomenclature

$B(\cdot\,\cdot)$	=	Beta function
C	=	boundary layer constant given in Table 1
C^*	=	boundary layer coefficient $\equiv Nu_x/(\mathrm{Pr}^\gamma \mathrm{Re}_x^\beta)$
C''	=	constant given in Eqs. (13) and (15)
h	=	heat transfer coefficient, $W/(m^2 \cdot K)$
I	=	given in Eqs. (14) and (16)
k	=	thermal conductivity, $W/(m \cdot K)$
L	=	total board length in x-direction, m
N	=	total number of heat sources
q	=	heat flux density, W/m^2
Q	=	heat flow rate, W
R	=	thermal resistance, $°C/W$
t	=	total board thickness in z-direction, m
T	=	temperature, $°C$
u, U	=	approach velocity in the x-direction, m/s
W	=	total board width in y-direction
x, y, z	=	Cartesian coordinates

Dimensionless Parameters

Bi	=	Biot Number $\equiv \dfrac{h \cdot t}{k_s}$
Nu_x	=	Local Nusselt Number $\equiv \dfrac{h \cdot x}{k_f}$
Pr	=	Prandtl number $\equiv \dfrac{\nu}{\alpha} = \dfrac{c_p \cdot \mu}{k_f}$
Re_x	=	Local Reynolds Number $\equiv \dfrac{U \cdot x}{\nu} = \dfrac{U \cdot \rho \cdot x}{\mu}$

Greek Symbols

α	=	thermal diffusivity $\equiv k_f/(\rho \cdot c_p)$, m^2/s
β	=	Reynolds number exponent
γ	=	Prandtl number exponent
$\Gamma(\cdot)$	=	gamma function
δ	=	hydraulic boundary layer thickness, m
δ_t	=	thermal boundary layer thickness, m
ϵ	=	thermal radiation emissivity
θ	=	temperature excess, $T - T_\infty$, $°C$
μ	=	dynamic viscosity, $kg/(m \cdot s)$
ξ	=	dummy variable in x flow direction, m
ρ	=	density, kg/m^3
σ	=	Stefan-Boltzmann constant $\equiv 5.67 \times 10^{-8}$, $W/(m^2 \cdot K^4)$
χ	=	dimensionless position, ξ/x
χ''	=	$1 - \chi^a$
∇	=	Laplacian operator in Cartesian coordinates

Subscripts

b	=	board (PCB) level at a package
c	=	package casing exposed to fluid cooling
f	=	fluid
H	=	harmonic mean
i	=	a particular layer in a multi-layered PCB
M	=	total number of layers in a multi-layered PCB
P	=	effective parallel heat flow path
s	=	solid
S	=	effective series heat flow path
w	=	wall
∞	=	free stream

Introduction

Electrical and mechanical engineers have long been aware of the potential thermal related reliability problems associated with high powered, high density electronic circuitry. Circuit designers have traditionally used prototype testing to monitor the thermal response of new circuit designs. But the prohibitive cost of prototype development, both in terms of financial investment and in terms of time to deliver the finished product to market restrict the designer in his ability to develop an optimized thermal design. During the early stages of the design process the circuit designer is primarily concerned with determining the sensitivity of board temperatures to changes in basic design parameters, such as the thermal conductivity of the board, flow velocity and package location. The overall accuracy of the predicted temperature distribution is important, but it is of lesser importance than model versatility, especially the ability to predict fundamental trends with a minimum of setup and execution time. It is to this end that META (MicroElectronic Thermal Analyser), the simulation routine presented in this paper, is addressed.

Commercially available thermal analysis codes for microelectronic applications generally fall into two categories. The first category encompasses those tools which offer advanced computer graphic displays for both input and output but contain weak analysis routines, which are primarily based on "rule-of-thumb" solutions and generalized correlations. In an effort to reduce the complexity of the analysis, these codes are based on many simplifying assumptions which also reduce the physical significance of the problem being modeled. The second category of codes involve large, elaborate finite difference or finite element based methods which allow for complex geometries and boundary conditions. These methods involve approximating the governing equations over a small domain reducing the problem to a simple system of linear algebraic equations with a finite number of unknowns. However, a full three-dimensional discretization, especially for an electronics circuit board with an aspect ratio of greater than 150:1, could require more than 200 000 elements to adequately discretize the circuit board and the air stream. The time and the cost of obtaining a converged solution using these methods is beyond what can be accepted as a commercial design tool. Additionally, the input data required by these programs is rarely known to a similar level of accuracy as the projected accuracy of the solution, introducing further uncertainty into a solution which might normally be perceived as highly accurate.

The need for a thermal analysis tool which incorporates many of the capabilities of the elaborate numerical codes but with design flexibility, speed of execution and low operating cost is required. The approach chosen in this work is to use analytical solutions as much as possible, but where analytical techniques are not feasible, a combination of numerical and analytical solutions will be used. An analytical approach helps preserve the physical aspects of the problem and in many instances reduces the time required to obtain a solution.

A microelectronic circuit board, as shown in Fig. 1, has a complex temperature field, established through the thermal interaction of many discrete heat sources with a multilayer circuit board and the boundary layer, which may be laminar or turbulent, depending on the nature of the flow. The complexity of the temperature field is also reflected in the governing equations describing the thermal behavior, and as such an exact analytical solution is not available with present solution techniques. However, approximate methods, which significantly simplify the solution technique, can be used to obtain accurate solutions to highly complex conjugate heat transfer problems.

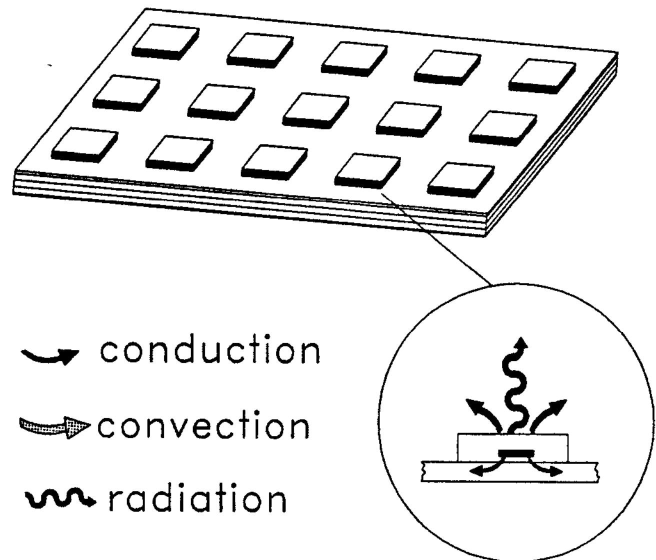

Figure 1: Typical PCB Showing Heat Transfer Paths and Package Components

META combines an analytical boundary layer solution with a finite volume solid body solution, which takes advantage of the negligible temperature gradient across the thickness of a circuit board (i.e. $Bi < 0.1$), thereby allowing a two-dimensional solution to be used to solve for board temperatures. The boundary layer solution is based on existing solution methods for laminar and turbulent boundary layer flows over flat plates where the integral form of the boundary layer equations are solved given a flux specified boundary condition. The resulting formulation for the local Nusselt number is

then used as the surface convective condition in the solid body model, as presented by Culham and Yovanovich (1987). The solution methods for solving the energy equation in the fluid and the solid domain are modified to accommodate arbitrarily specified surface heat flux. The two solutions are coupled using an iterative procedure to give a unique temperature profile at the fluid-solid interface which simultaneously satisfies the energy equation in both the fluid and the solid domains.

Assumptions

Surface mount technology eliminates the need to install component pins in pre-formed through-holes which must be filled with solder to provide electrical and mechanical integrity. Instead, components are soldered to pads on the surface of the circuit board known as "foot prints". Surface mount technology permits components to be mounted closer to the surface of the circuit board, giving the overall surface of the circuit board a smooth appearance. The upper surface of the component packages will be considered flush with the surface of the circuit board.

The circuit board aspect ratio, defined as the total length of the board in the flow direction (x) over the thickness of the board (L/t), is typically of the order of 150:1. The predominant surfaces for convective cooling are the upper and lower surfaces of the circuit board, which encompass approximately 99% of the total exposed surface area of the board. Therefore, the heat transfer through the edges of the board is considered negligible and these surfaces will be treated as adiabatic in all subsequent analyses.

Although the convective heat transfer coefficient varies significantly over the surface of an electronic circuit board, typical values of the Biot Number ($Bi = ht/k_s$) range from 0.0003 to 0.1. The magnitude of the Biot number serves as an indication of the relative magnitude of the thermal resistance across the thickness of the board to the thermal resistance within the fluid boundary layer. Since it is commonly accepted that a $Bi < 0.1$ allows a one-dimensional conduction analysis to be used with minimal deviation from results obtained using a more rigorous two-dimensional solution, a two-dimensional spatial solution (x, y) will be used in the iterative model as opposed to a fully three-dimensional solution.

The cooling fluid is taken to be dry air with flow over the circuit board assumed to be steady, two-dimensional and incompressible. The maximum flow velocity anticipated in microelectronic applications is low enough that frictional dissipation can be considered negligible. Since the component packages are assumed to be flush mounted the pressure difference through the boundary layer can be assumed uniform.

The circuit board is assumed to have a uniform thickness with heat dissipating component packages being in intimate contact with the surface of the circuit board. The power dissipated by the components is assumed to be steady and invariant with respect to time.

Solution Procedure

The fluid-side analysis will use a solution to the energy-momentum boundary layer equation (Tribus and Klein (1952)),

$$\frac{d}{dx}\int_0^{\delta_t} uT_f dz = -\alpha\frac{\partial T_w}{\partial z} \quad (1)$$

which has an unknown fluid velocity u in the x-direction, temperature T_f, and wall temperature gradient $\partial T_w/\partial z$. The solid-side temperature field $T_s(x, y)$ must satisfy

$$\nabla^2 T_s - \frac{h}{kt}T_s - S = 0 \quad (2)$$

with $h \equiv h(x, y)$ being the fluid film coefficient locally specified on top of the board surface; S represents heat source terms; k is the effective board thermal conductivity, and t is the overall board thickness in the z-direction. A standard, finite volume or control volume based, finite element discretization of Eq. (2), as described in Minkowycz *et al* (1988), will allow for the local specification of h and S. Equation (1) could also be similarly discretized, but instead, further suitable approximations for u, T_f will reduce Eq. (1) to an integral expression for θ_s in terms of the wall heat flux q_w. This is described in the following subsection.

Specifying h, S, Eq. (2) will determine the temperature excess field θ_s, and q_w, the heat flux entering the fluid. This q_w is then used in the fluid-side equation to determine θ_f, and hence a new estimate of h. An iterative procedure to converge $\theta_f \to \theta_s < tol$ is then implemented between the two solutions. Equation (2) assumes that the backside of the board is insulated; if cooling exists on the backside as well, then the h in Eq. (2) will be a sum of top and bottom film coefficients.

Boundary Layer Model. A forced convection heat transfer analysis of flow past a flat plate can be easily obtained for an isothermal boundary condition using one of a variety of techniques, including an exact similarity solution as originally formulated by Blasius (1908). However, the analysis for a non-isothermal boundary condition is not as straightforward, and very often it is necessary to use approximate methods such as von Kármán's integral technique. Arbitrary distributions of either temperature or heat flux can be approximated as a series of step changes, where individual step change solutions are superimposed to provide a means for calculating the local heat flux or the fluid temperature adjacent to the wall. The convective heat transfer coefficient can be derived by developing the integral form of the boundary layer equations in terms of two axial position variables, ξ and x, where

$$0 \le \xi \le x \; ; \; 0 \le x \le L \quad (3)$$

plus known thermophysical parameters and flow conditions. The example of laminar, incompressible flow over a flat plate, where the wall temperature is expressed as a single step change and the boundary layer velocity and temperature profiles are expressed in terms of

a cubic parabola, is well documented (Eckert and Drake, 1959) and the local convective heat transfer coefficient is given as

$$h(\xi, x) = 0.332\frac{k_f}{x}\mathrm{Pr}^{1/3}\mathrm{Re}_x^{1/2}\left[1-\chi^{3/4}\right]^{-1/3} \tag{4}$$

where $\chi = \xi/x$.

The local heat flux can be evaluated by substituting Eq. (4) into

$$q_w = \int_{\xi=0}^{x} h(\xi, x)d\theta_f(\xi) \tag{5}$$

where θ_f denotes the temperature excess of the fluid immediately adjacent to the wall.

The general form of Eq. (4) can be written in terms of five parameters as

$$h(\xi, x) = C\frac{k_f}{x}\mathrm{Pr}^{\gamma}\mathrm{Re}_x^{\beta}[1-\chi^{a}]^{-b} \tag{6}$$

where the parameters (namely C, γ, β, a and b) will change subject to the flow conditions and the type of solution technique used in the analysis.

Table 1 is a non-exhaustive list of constants used in Eq. (6) for laminar and turbulent flow over a flat plate.

Table 1: Constants Used in Eq. (5) for Laminar and Turbulent Flow

solution	C	γ	β	a	b	reference
laminar						
exact†	0.332	1/3	1/2	3/4	1/3	Eckert (1950)
approximate	0.304	1/3	1/2	3/4	1/3	Rubesin (1945)
approximate	0.323	1/3	1/2	3/4	1/3	Kays (1966)
turbulent						
approximate	0.0288	1/3	4/5	39/40	7/39	Rubesin (1951)
approximate	0.0289	1/9	4/5	9/10	1/9	Seban (1951)

† parameters C, γ, and β are determined from the exact solution of Blasius (1908)

The bracketed term in Eq. (6) is referred to as a delay factor and can be thought of as a weighting function based on the proximity of the step change in temperature in relation to the location at which the heat flux is being calculated.

The above expressions are all based on the premise that the boundary condition is temperature specified and the heat flux at the wall is to be calculated. However, many applications exist for which the heat flux is known and the wall temperature is the unknown quantity. Heat flux specified problems necessitate that the expression for the convective heat transfer coefficient, as given in Eq. (4), be derived either by returning to the integral form of the boundary layer energy equation or by inverting the solution to the temperature specified problem.

The local heat flux for a flat plate with a temperature specified boundary condition can be written as

$$q_w = \int_{\xi=0}^{x} C\cdot\frac{k_f}{x^{(1-\beta-ab)}}\mathrm{Pr}^{\gamma}\left(\frac{\rho u}{\mu}\right)^{\beta}[x^a-\xi^a]^{-b}\,\theta_f(\xi)d\xi \tag{7}$$

Recognizing that Eq. (7) is in the form of a Volterra integral of the first kind, allows the equation to be inverted, thus allowing local temperature excess to be written in terms of the wall heat flux.

$$\theta_f(x) = \frac{\mathrm{Pr}^{-\gamma}\mathrm{Re}_x^{-\beta}x}{\Gamma(b)\Gamma(1-b)(C\cdot k_f)}\int_0^1 q_w\left[1-\chi^a\right]^{-(1-b)}d\chi \tag{8}$$

If the heat flux, q_w, is assumed uniform over each discretized section, Eq. (8) can be solved in terms of Beta functions, to give

$$\theta_f(x) = \frac{\mathrm{Pr}^{-\gamma}\mathrm{Re}_x^{-\beta}x}{\Gamma(b)\Gamma(1-b)\ (C\cdot k_f)}\sum_{i=1}^{N} q_{w_i}\left(B_{\chi_{i-1}''}(b,1/a)-B_{\chi_i''}(b,1/a)\right) \tag{9}$$

As shown by Sparrow and Lin (1965), the integral form of the energy equation can also be solved using a flux specified boundary condition to produce a slightly different form of Eq. (8).

$$\theta_f(x) = \frac{\mathrm{Pr}^{-\gamma}\mathrm{Re}_x^{-\beta}\ x}{\frac{1}{b}(C^*\cdot k_f)}\int_0^1 q_w\left[1-\chi\right]^{-(1-b)}d\chi \tag{10}$$

where C^* is given in Table 2 for different velocity and temperature profiles.

Although the solution to Eqs. (8) and (10) lead to essentially identical results, the slight difference in the form of the delay factor provides a tremendous simplification in the solution procedure. In the flux specified solution of Sparrow and Lin (1965), χ is always raised to the first power, regardless of the flow regime used in the solution technique. This is of mathematical significance because it simplifies the integral and allows a solution to be obtained without the use of incomplete Beta functions. If q_w is assumed to be a step-wise uniform function of x, the integral in Eq. (10) can be evaluated easily to give

$$\int_0^1 [1-\chi]^{-(1-b)}d\chi = -\frac{1}{b}[1-\chi]^b\Big|_0^1 \tag{11}$$

which can also be written in terms of an incomplete Beta function as

$$\int_0^1 [1-\chi]^{-(1-b)}d\chi = B_1(b,1) \tag{12}$$

Solutions for non-uniform distributions of heat flux, such as ramps and parabolic distributions, can be obtained (Culham, 1988), if q_w is known in terms of an integrable form of χ. However, the practical applicability of these solutions is limited since the heat flux distribution of many microelectronic applications is not known *a priori*, but instead is a function of thermophysical properties, flow conditions and geometry. A boundary layer model must be able to adapt to local conditions, including arbitrary changes in the heat flux distri-

Table 2: Dimensionless Parameters for Various Velocity Profiles in Laminar Flow

Velocity and Temperature Profile	$\frac{\delta}{x}\sqrt{\mathrm{Re}_x}$	$\frac{\delta_t}{x}\sqrt{\mathrm{Re}_x}\sqrt[3]{\mathrm{Pr}}$	C^* $\frac{Nu_x}{\sqrt{\mathrm{Re}_x}\sqrt[3]{\mathrm{Pr}}}$
Exact	5.00	—	0.454†
Linear, η	3.46	2.75	0.364
Quadratic, $\frac{3}{2}\eta - \frac{1}{2}\eta^3$	4.64	3.59	0.417
Sinusoidal, $\sin\left(\frac{\pi}{2}\eta\right)$	4.80	3.70	0.424

† obtained by inverting the temperature based solution

bution, if the thermal behavior of a populated microelectronic circuit board is to be accurately modelled. Multiple localized solutions can be superposed to obtain the temperature profile over the full length of the circuit board.

Discretized Solution. The heat flux distribution in most conjugate heat transfer applications does not conform to one of the simple distributions, such as a ramp or a parabolic. If the heat flux distribution is known as a function of x, numerical integration can be used to obtain a solution to the integral in Eq. (10). However, the dependence of the heat flux on the temperature field within the solid does not guarantee a distribution over each heat source which is easily represented as a function of χ. Instead a method of discretizing the plate into elements, which are sufficiently small to allow the heat flux calculated at the midpoint of the element to be representative of the heat flux over the full width of the element, will be used to express the actual heat flux distribution as a series of finite steps. In the limit, as the element size becomes infinitesimally small, the step profile in heat flux approaches the actual heat flux distribution.

Regardless of the method used to obtain a temperature solution, a general formulation for the localized temperature excess, given a piecewise step-change in heat flux, can be written as follows:

$$\theta_f(x) = \left\{\frac{\mathrm{Pr}^{-\gamma}\mathrm{Re}_x^{-\beta}x}{C'' \cdot k_f}\right\}\sum_{i=1}^{N}[q_{w_i}\mathcal{I}_i] \quad (13)$$

where for $a \neq 1$

$$C'' = \frac{1}{a}\Gamma(b)\Gamma(1-b)\cdot C \quad (14)$$

$$\mathcal{I}_i = \frac{1}{a}\left\{B_{1-\chi_{(2i-1)}}(b,1/a) - B_{1-\chi_{(2i)}}(b,1/a)\right\} \quad (15)$$

and for $a = 1$

$$C'' = \frac{1}{b}\cdot C^* \quad (16)$$

$$\mathcal{I}_i = \frac{1}{b}\cdot\left\{[1-\chi_{(2i-1)}]^b - [1-\chi_{(2i)}]^b\right\} \quad (17)$$

Solid-Side Model. The control-volume based finite element approximation of Eq. (2) is incorporated by **META** as the solid-side PCB solver scheme. Although the PCB medium is modelled as a single homogeneous substrate, with thermal conductivity k, a supplementary study by Lemczyk et al., (1991) has shown that a multi-layered printed circuit board can be quite accurately modelled using a harmonic-mean effective thermal conductivity, k_H. This is given by

$$k_H = 2\left(\frac{1}{k_P} + \frac{1}{k_S}\right)^{-1} \quad (18)$$

where

$$k_P = \sum_{i=1}^{M}(k_i t_i) / \sum_{i=1}^{M} t_i \quad (19)$$

$$k_S = \sum_{i=1}^{M} t_i / \sum_{i=1}^{M}(t_i/k_i) \quad (20)$$

for an M-layered PCB, where each i-layer has a thermal conductivity k_i and thickness t_i. Although there will be some error associated with actual temperature prediction across the PCB using this approximation, it was shown that the PCB thermal resistance R_{bf} can be accurately predicted.

Fluid-Solid Coupling. The two models described above can be coupled to solve conjugate problems by iterating between each solution. The local heat transfer coefficient, which is calculated in the fluid side model, is used as input to the solid side model. Similarly, the surface heat flux, which is calculated in the solid side model, is used as input to the fluid side model. A flow chart of the iterative procedure used to model conjugate heat transfer is given in Fig. 2.

The iterative model is initiated by assuming a heat flux distribution over the surface on which the heat sources are placed. Typically, the heat flux is assumed uniform over the heat sources and zero at all non-source locations. On each successive iteration the heat flux is redistributed in a manner which forces the temperature difference, between the wall and the fluid immediately adjacent to the wall, towards zero. The solution is considered to be converged when the difference between the fluid and solid temperature is less than a user specified tolerance. The arithmetic mean of the two "converged" temperatures is used as the final wall temperature solution.

Model Enhancements. The basic conjugate model described in the previous sections calculates the surface temperature profile for air flow over a flat plate suspended in a free stream. Most microelec-

tronic configurations do not conform to this relatively simple model and as such certain enhancements must be incorporated in order to more closely simulate practical applications. Controlled empirical testing has been used to isolate many of these secondary effects, such as radiative heat transfer, channel effects, natural convection, mixed convection and contact resistance, in order to ascertain the relative importance of each with respect to overall heat transfer. In all instances elaborate analytical modeling and the judicious use of simplifying assumptions have allowed modules to be developed which operate within the basic conjugate model described above to provide the modeling enhancements which simulate microelectronic applications. The following sections will be used to define the governing equations for each of the modeling enhancements but will not attempt to detail the indepth analysis leading up to the equations. Where background publications are available, they will be referenced, where publications are not presently available, readers are asked to watch for future publications by the Microelectronics Heat Transfer Laboratory which will provide the analytic background.

Natural Convection. The delay factor for forced convection and a flux specified boundary condition is given in Eq. (10) as $[1-\chi]^{-(1-b)}$. Natural convection applications exhibit a different weighting factor (Lee and Yovanovich, 1991) and the delay factor can be written as

$$[1-\chi]^{-(1-b)+1/10} \tag{21}$$

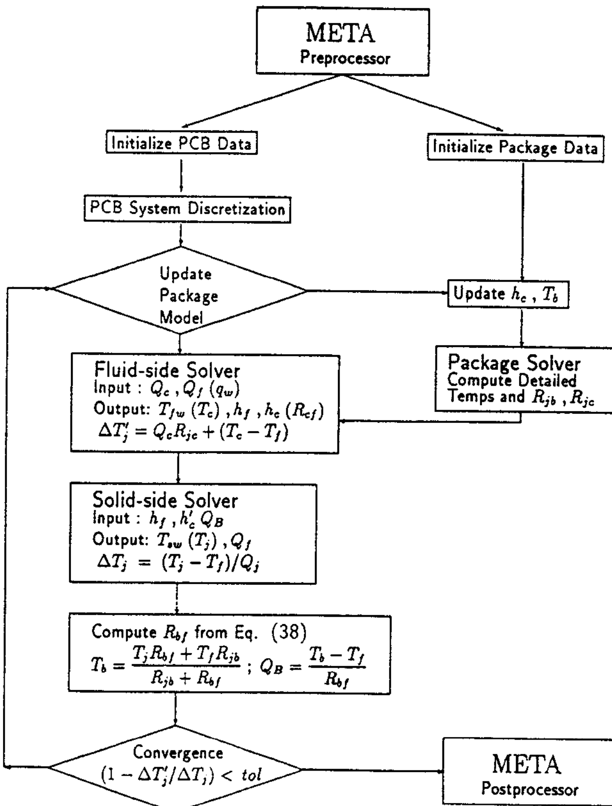

Figure 2: Flow Chart for META Iterative Solution Procedure

The effective natural convection velocity, which can be used in the Reynolds number of the forced convection expression (13), becomes

$$U = \frac{(C_f \cdot f_l)^2 \cdot \mathrm{Ra}^{2/5} \cdot \nu}{\mathrm{Pr}^{2/3} \cdot x} \tag{22}$$

where

$$C_f = 1/C^* = 2.203 \tag{23}$$

$$f_l = \left(\frac{\mathrm{Pr}}{4 + 9 \cdot \sqrt{\mathrm{Pr}} + 10 \cdot \mathrm{Pr}}\right)^{1/5} \tag{24}$$

and

$$\mathrm{Ra} = \frac{g \cdot Q \cdot \mathrm{Pr} \cdot x^3}{T_\infty \cdot k_f \cdot \nu^2} \tag{25}$$

The accumulated heat flow, Q, into the air stream from the leading edge of the plate up to the point where the flow velocity (attributed to natural convection) is being calculated, is given as

$$Q = \int_0^x q\,dx \tag{26}$$

Mixed Convection. The Nusselt number for mixed convection can be written in terms of two components representing the Nusselt numbers for forced and natural convection when the boundary conditions are uniformly specified.

$$\mathrm{Nu}_m^3 = \mathrm{Nu}_f^3 + \mathrm{Nu}_n^3 \tag{27}$$

Since the Nusselt number is proportional to the square root of the flow velocity

$$\mathrm{Nu}_f \propto \sqrt{\mathrm{Re}} \propto \sqrt{u} \tag{28}$$

an effective mixed convection velocity can be written in terms of two component velocities as follows

$$u_m^{1.5} = u_f^{1.5} + u_n^{1.5} \tag{29}$$

where u_f is the induced stream velocity and u_n is given by Eq. (22). Due to the dependence of the delay function on the type of convective heat transfer, an interpolation between the two values used for forced and natural convection, as shown in Fig. 3, can be accurately used to determine the exponent on the delay factor.

Radiative Heat Transfer. For many low temperature applications (less than 400 K), radiative heat losses are considered negligible and generally neglected. However, an examination of a heat transfer coefficient attributed to radiative heat losses, as given in Eq. (30), reveals that for temperatures only marginally above room temperature (293 K), a radiative heat transfer coefficient of order 5 $W/(m^2 \cdot K)$ is common. Figure 4 shows the radiative heat transfer coefficient for a temperature rise above ambient between 0.1 and 100 K.

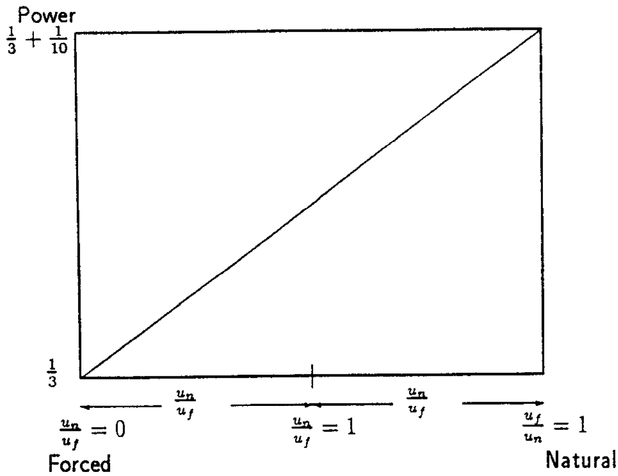

Figure 3: Interpolation Curve for Exponential Factor in the Delay

$$h_r = \sigma\epsilon\left(T^4 - T_\infty^4\right)/(T - T_\infty) \tag{30}$$

Typical convective heat transfer coefficients may range between $5\ W/(m^2 \cdot K)$ for natural convection up to $50\ W/(m^2 \cdot K)$ for low velocity forced convection applications with air cooling. Over this range of convective heat transfer coefficients, the radiative component can be between 5 and 50 percent of the overall heat transfer mechanism. Such an amount is far from negligible and must be considered in microelectronic applications, especially those applications where a single card is being cooled and a canceling effect between similar parallel cards is not obtained.

Two approaches can be used to account for radiative heat losses. The first is to calculate the local radiative heat flux, as given in Eq. (31), and add this value to the heat loss in the solid body model.

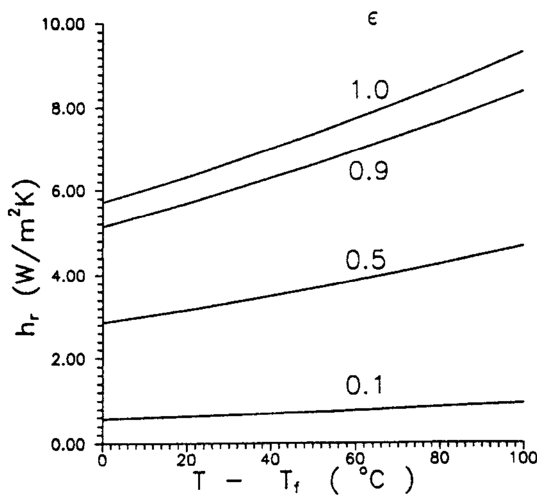

Figure 4: Radiative Heat Transfer Coefficient

$$q_r(x) = \sigma\epsilon\left(T_s^4 - T_\infty^4\right) \tag{31}$$

The fluid-side model is transparent to radiative losses and no accounting for $q_r(x)$ is made in the boundary layer model.

The second approach involves calculating the total local heat flux dissipated at the surface of the solid as follows

$$q_t(x) = h_t(x)(T_s - T_\infty) \tag{32}$$

It follows then that by combining Eqs. (31) and (32), the heat flux dissipated into the boundary, and in turn used in the fluid-side model is

$$q_c = q_t - q_r \tag{33}$$

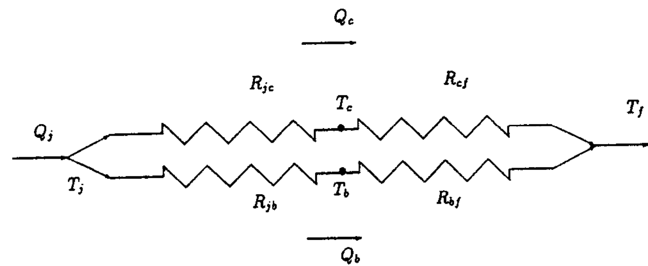

Figure 5: Package Resistance Network

Package Modelling and Thermal Resistances

For every electronic package mounted on a PCB, a thermal resistance network as shown in Fig. 5 will be used. An overall junction-to-ambient resistance (R_{ja}) for any particular component can be determined from the formula

$$R_{ja} = \frac{T_j - T_f}{Q_j} = \left(\frac{1}{R_{jc} + R_{cf}} + \frac{1}{R_{jb} + R_{bf}}\right)^{-1} \tag{34}$$

where

$$R_{jb} = \frac{T_j - T_b}{Q_b} \tag{35}$$

$$R_{jc} = \frac{T_j - T_c}{Q_c} \tag{36}$$

$$R_{cf} = \frac{T_c - T_f}{Q_c} \tag{37}$$

$$R_{bf} = \frac{T_b - T_f}{Q_b} \tag{38}$$

In the above, the temperatures are all mean values. T_j represents the average die-junction temperature within a package, T_c is the average case temperature of the package (which is directly exposed to the cooling fluid), and T_b is the average board temperature directly beneath the package. Q_j is the applied total heat flow rate to the package junction, a specified quantity; Q_b and Q_c are respectively the total heat flow rates to the board and to the package casing. If the package resistances are assumed to be negligible, i.e. $R_{jc} \equiv R_{jb} \equiv 0$, then the junction T_j, case T_c, and board T_b are equivalent; this

represents a flush-mounted heat source on the printed circuit board. When R_{jb} and R_{jc} have non-zero, finite values, then the fluid-side and solid-side solvers in **META** will establish $T_{fw} \rightarrow T_c$ and $T_{sw} \rightarrow T_b$. The iterative convergence strategy used is described in Lemczyk et al., (1989), and is also illustrated in Fig. 2. It is important to note from Fig. 2 that the fluid-side solver will compute the fluid at-wall temperature T_{fw} and the case temperature T_c at a package location. The solid-side solver computes T_{sw}, but this represents the junction temperature T_j estimate; the associated film coefficient is based on inclusion of the junction to case thermal resistance, i.e.

$$h_c' = \frac{1}{A_c(R_{jc} + R_{cf})} \tag{39}$$

where A_c represents the total package case area exposed to fluid cooling. Also, not clearly shown in Fig. 2 is the radiation heat transfer component from the PCB, but this is incorporated in the q_w input of the fluid-side solver.

A microelectronic package modeller, as utilized by **META**, and described in Lemczyk et al., (1989), will determine R_{jb}, R_{jc}, readily given as input the average film coefficient over the package h_c and the average board temperature T_b where the package is attached. **META**, as a PCB analyzer, requires values of R_{jb}, R_{jc} as input parameters, and will determine R_{cf}, hence h_c, and R_{bf}, hence T_b as output. So one can see that the non-linear nature by which the solution procedure is described will require iteration between the package model solver and the PCB solver. Since the PCB solver does not discretize the package die plane adequately to model the actual die location, the establishment of T_j and an accurate package thermal description can only be obtained from the package modeller. This would incorporate the average fluid film coefficient obtained from the PCB modeller. The PCB modeller will, however, accurately predict local thermal behaviour for temperature and heat flux levels at non-source locations. It is only when $R_{jb}, R_{jc} > 0$, that thermal predictions are determined at a package (source) location on an average basis.

Although the above discussion concerns a single-chip package (SCP) description, multi-chip packages (MCPs) are also easily modelled by the **META** package modeller (Lemczyk et al., 1989). For an MCP, the mean quantities in (34) to (38) would represent an averaged die-plane chip temperature, which would enter the PCB analysis. However, the detailed individual chip temperatures would still be locally computed by the package modeller.

Meta Simulation Test Case

Figure 6 illustrates a sample experimental PCB which was simulated by **META**. A total of 69 square power modules were mounted on the PCB, and supplied with varying power levels in columns as shown. Several different power configurations were simulated; for the one shown, the experimentally measured temperatures of each package are noted on each module. The heat source modules were

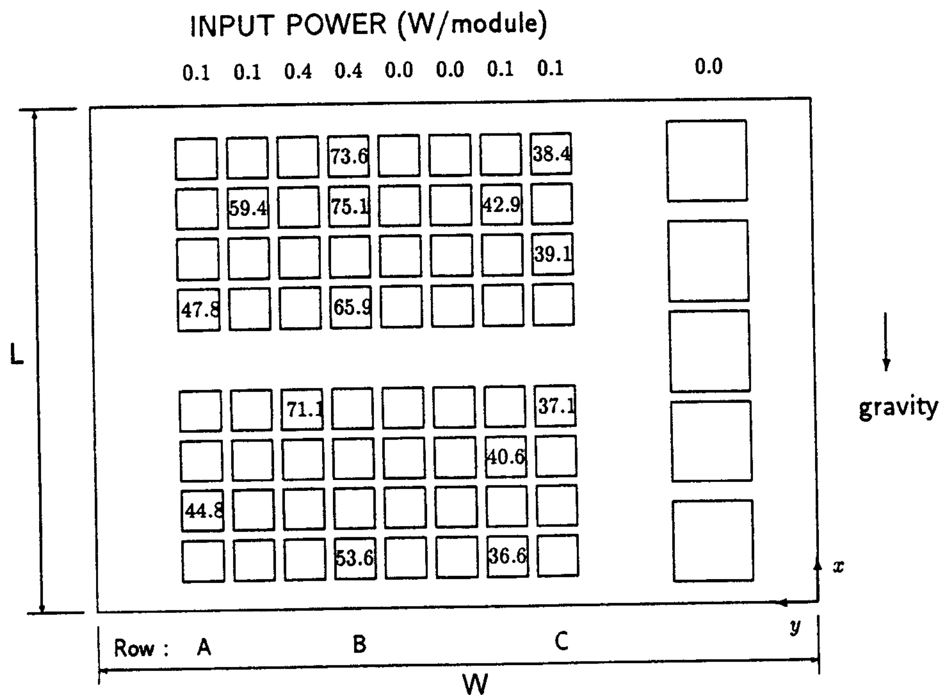

Figure 6: Experimental PCB With Powered Modules and Measured Temperatures

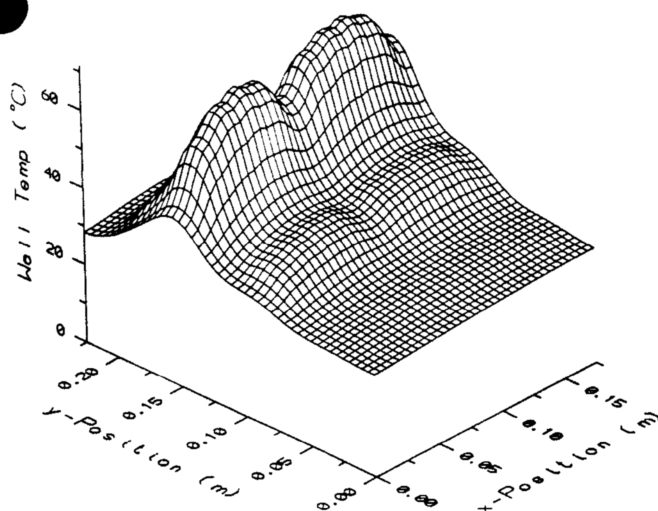

Figure 7: Predicted PCB Temperatures by META

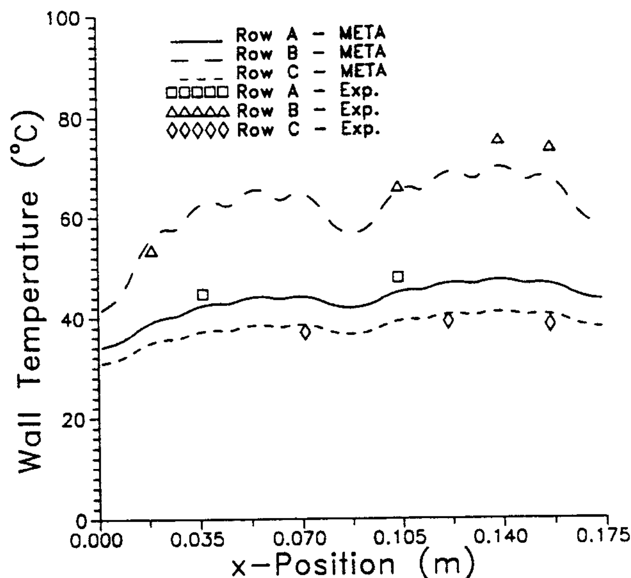

Figure 8: Experimental vs. META Temperatures

modelled as having no internal resistance, i.e., R_{jb}, $R_{jc} \equiv 0$, since pertinent details concerning package construction were not given by the supplier. The PCB had a thickness of $t = 2.5$ mm, with effective thermal conductivity $k = 6.24$ W/mK, board length $L = 175$ mm, and board width $W = 228$ mm. The PCB radiation emissivity was $\epsilon = 0.824$ and the individual package emissivity was $\epsilon = 0.073$. The PCB was exposed to natural convection cooling conditions only, with no external velocity U_∞ supplied; the gravity vector is shown in Fig. 6. The ambient air temperature was $T_\infty = 22.7°C$.

Figures 7 and 8 give results obtained using META compared with those experimentally supplied for the PCB. Figure 7 is a contour plot showing predicted temperature levels over the entire PCB. Since two columns of package modules were not supplied with power, as shown by Fig. 6, there is a slight dip in the temperature contour of approximately $10°C$. Figure 8 illustrates a direct comparison between experimental temperatures and those simulated by META along x-strips at specific centered row y-locations along the width of the PCB.

Conclusions

In this paper a conjugate fluid-solid model for PCB thermal analysis has been described. The computer simulation code, META, utilizes this theory and has provided good agreement with experimental results. The inclusion and description of a package modeller within META has also been outlined, detailing the importance of thermal resistances in accurately calculating local chip temperatures within a package.

Acknowledgements

The authors would like to gratefully acknowledge support from the Natural Sciences and Engineering Research Council of Canada under Operating Grant No. 661-062/88, and also to Bell Northern Research, Kanata, Ontario, and IBM Corporation, Poughkeepsie, New York.

References

Bayley, F.J., Owen, J.M. and Turner, A.B., 1972, *Heat Transfer*, Thomas Nelson and Sons Ltd., London.

Blasius, H., 1908, "Grenzschichlen in Flüssigkeiten mit kleiner Reibung", *Z. Math. Phys.* 56, 1. [English translation in NACA Technical Memo Number 1256]

Culham, J.R., 1988, *Conjugate Heat Transfer From Surfaces With Discrete Thermal Sources*, Ph.D. Thesis, University of Waterloo, Waterloo, Canada.

Culham, J.R. and Yovanovich, M.M., 1987, "Non-Iterative Technique for Computing Temperature Distributions in Flat Plates with Distributed Sources and Convective Cooling", Second ASME-JSME Thermal Engineering Joint Conference, Honolulu, Hawaii, March 22-27.

Eckert, E.R.G., 1950, *Introduction to the Transfer of Heat and Mass*, McGraw-Hill Book Company, Toronto.

Eckert, E.R.G. and Drake, R.M. Jr., 1959, *Heat and Mass Transfer*, McGraw-Hill Book Company, Toronto.

Karvinen, R., 1978, "Some New Results For Conjugated Heat Transfer In A Flat Plate", *Int. J. H. Mass Transfer*, Vol. 21, pp. 1261-1264.

Kays, W.M., 1966, *Convective Heat and Mass Transfer*, McGraw-Hill Book Company, Toronto.

Lee, S., and Yovanovich, M.M., 1991, "Linearization of Natural Convection From a Vertical Plate With Arbitrary Heat Flux Distributions," to be presented at the 1991 ASME Winter Annual Meeting, Atlanta, Georgia, December 1-6.

Lemczyk, T.F. and Culham, J.R., 1989, " Thermal Analysis of Electronic Package Components," MHTL Reports G-27,G-28, University of Waterloo, Waterloo.

Lemczyk, T.F., Mack, B., Culham, J.R., and Yovanovich, M.M., 1991, "PCB Trace Thermal Analysis and Effective Conductivity", submitted to the ASME Journal of Electronic Packaging; presented at the Seventh IEEE SEMI-THERM Symposium, Phoenix, AZ, February 12-14.

Minkowycz, W.J., Sparrow, E.M., Schneider, G.E., Pletcher, R.H., 1988, *Handbook of Numerical Heat Transfer*, John Wiley & Sons Inc., New York.

Rubesin, M.W., 1945, *An Analytical Investigation of the Heat Transfer Between a Fluid and a Flat Plate Parallel to the Direction of Flow Having a Stepwise Discontinous Surface Temperature*, M.S. Thesis, University of California, Berkeley.

Rubesin, M.W., 1951, "The Effect of an Arbitrary Surface Temperature Variation Along a Flat Plate on the Convective Heat Transfer in an Incompressible Turbulent Boundary Layer", NACA Technical Note 2345.

Seban, R.A., 1950, "Calculation Method for Two-Dimensional Boundary Layers With Arbitrary Free Stream Velocity Variation and Arbitrary Wall Temperature Variation", Inst. of Engrg. Res., University of California, Berkeley.

Simeza, L.M., 1986, "Application of the Finite Volume Method to Conjugate Heat Transfer in Electronic Devices", MHTL Technical Report G-16, Microelectronics Heat Transfer Laboratory, University of Waterloo, Waterloo, Ontario.

Sparrow, E.M. and Lin, S.H., 1965, "Boundary Layers With Prescribed Heat Flux — Applications To Simultaneous Convection and Radiation", *Int. J. H. Mass Transfer*, Vol. 8, pp. 437-448.

Tribus, M. and Klein, J., 1952, "Forced Convection from Non-Isothermal Surfaces", Heat Transfer Symposium, Engineering Research Institute, University of Michigan.

von Kármán, Th., 1921, "Über laminare und turbulente Reibung", *ZAMM*, Vol. 1, No. 4, pp. 233-252. [English translation in NACA Technical Memo 1092]